DOI: 10.18721/JPM.14108
UDC 537.533.2, 598.9

LOW-FIELD ELECTRON EMISSION FROM THIN FILMS OF METALS

I.S. Bizyaev, P.G. Gabdullin, N.M. Gnuchev, A.V. Arkhipov

Peter the Great St. Petersburg Polytechnic University,
St. Petersburg, Russian Federation

The paper presents an experimental study of the low-threshold field electron emission from thin films of metals (Mo, W, Zr, Ni and Ti) deposited on silicon substrates by magnetron sputtering. Several samples of such films having effective thickness in the range 6 – 10 nm were capable of room-temperature electron emission in electric field with macroscopic intensity as low as a few kV/mm. Optimized thermofield treatment procedure further improved their emission properties reducing the threshold field by several times. AFM study revealed a correlation between film's emission properties and their surface topography. At the same time, no equally pronounced correlation of the emissivity with other characteristics of coatings (including the sort of the metal and the silicon substrate conductivity type) was detected. Results of the study witness in favor of two-temperature (or hot-electron) emission mechanism for the investigated coatings.

Keywords: field emission, thin film, atomic force microscopy, hot-electron emission

Citation: Bizyaev I.S., Gabdullin P.G., Gnuchev N.M., Arkhipov A.V., Low-field electron emission from thin films of metals, St. Petersburg Polytechnical State University Journal. Physics and Mathematics. 14 (1) (2021) 105–120. DOI: 10.18721/JPM.14108

НИЗКОПОРОГОВАЯ ПОЛЕВАЯ ЭМИССИЯ ЭЛЕКТРОНОВ ТОНКИМИ ПЛЕНКАМИ МЕТАЛЛОВ

И.С. Бизяев, П.Г. Габдуллин, Н.М. Гнучев, А.В. Архипов

Санкт-Петербургский политехнический университет Петра Великого,
Санкт-Петербург, Российская Федерация

В работе экспериментально исследованы эмиссионные свойства тонких пленок нескольких металлов (Mo, Ni, W, Ti и Zr), нанесенных на кремниевые подложки методом магнетронного распыления. При эффективной толщине 6 – 10 нм, многие образцы пленок показали способность эмитировать электроны при комнатной температуре в поле с макроскопической напряженностью порядка единиц В/мкм. Оптимизированная процедура термополевой обработки позволяла дополнительно активировать их эмиссионные свойства, снижая эмиссионный порог в несколько раз. Была выявлена корреляция эмиссионных свойств пленок с топографией их поверхности, определяемой методом атомно-силовой микроскопии (АСМ). При этом выраженной корреляции эмиссионной способности с прочими характеристиками покрытий (в том числе с видом металла и типом проводимости подложки) обнаружено не было. Полученные экспериментальные результаты свидетельствуют в пользу двухтемпературной («горячеэлектронной») модели эмиссионного механизма для изученных покрытий.

Ключевые слова: полевая эмиссия, тонкая пленка, атомно-силовая микроскопия, эмиссия горячих электронов

Ссылка при цитировании: Бизяев И.С., Габдуллин П.Г., Гнучев Н.М., Архипов А.В. Низкопороговая полевая эмиссия электронов тонкими пленками металлов // Научно-технические ве-

домости СПбГПУ. Физико-математические науки. 2021. Т. 14. № 1. С. 105–120. DOI: 10.18721/JPM.14108

Introduction

One of the attractive applications of nanostructured materials is their use as a part of cold (non-heated) cathodes of electronic devices. Currently, in practice, most often are used either metal (or silicon) tips or carbon nanotubes and similar fibers [1 – 5]. However, many researchers believe that cold emitters of electrons that do not have sharp points – with a relatively smooth emitter boundary [3 – 9] – are also promising, even though no practically competitive systems of this type have been proposed so far.

In one of the experimental types of cold cathodes studied since the 1960s [10 – 13], a nanostructured metal (or carbon) film on a dielectric substrate was used as the main element. The film is actually a set of microscopic metal (or carbon) islands. The current in the film between the electrodes deposited on top of it flows as a result of the tunneling transfer of electrons through the gaps separating the islands. In this case, electroluminescence and electron emission into the vacuum are observed. The mechanism of such emission has not been definitively determined, but, according to the most popular model [13 – 15], it includes the following processes:

hot electrons are emitted,

the electronic subsystem of the islands is heated by the current injected into them,

high electron temperature is maintained as a result of violation of the energy exchange between the electrons and the lattice, the last effect being characteristic of nanoscale objects.

The validity of this model was confirmed by the observation of emission while using non-current methods of pumping electron energy into islands – in particular, under the influence of infrared (IR) radiation [13, 16].

Another type of experimental samples possessing cold emittion was studied in [17 – 19]. It was shown that carbon "nano-island" films on silicon substrates are able to emit electrons at room temperature in sufficiently weak electrostatic fields (the macroscopic field intensity was about 1 V/m) and without any additional effects, such as surface current excitation. At the same time, there were neither areas with low work function, nor high-aspect elements of topography (points, fibers, etc.) on the surface.

To describe the emissivity of such films, we proposed a model [20, 21], which is largely similar to the hot electron model described above. The assumption of slow relaxation of hot carriers in nanostructures is also used in this model, but it is assumed that this slowness is a result of the peculiarities of the electronic structure of sp^2-hybridized carbon [22, 23].

The primary goal of this paper was to test experimentally the validity of the latter assumption. It was necessary to determine whether the cold electron emission in macroscopic electric field strength of about 1 V/m (without other external influences, such as the flow of surface current or IR irradiation) is possible only for carbon island films, or it will also be observed in case of metal films of similar structures.

Experimental

The samples of metal films were deposited on naturally oxidized substrates of doped silicon by magnetron sputtering using a HEX unit manufactured by Mantis Deposit (Great Britain). The substrates were pre-cleaned by ultrasonic treatment in an acetone solution. Then they were installed on the slide table of the growth chamber and subjected to additional thermal cleaning at a temperature of about 150 °C and residual gases pressure of 10^{-3} Pa. Before spraying the coating, the magnetron target was also cleaned: the substrates were covered with a special screen during the first five minutes of the sprayer operation. The capabilities of the installation made it possible to conduct the metal deposition process at a residual gas pressure of about 10^{-4} Pa, to regulate the dep-

osition rate (from 0.13 to 1.0 Å/s) and the temperature of the substrates (from room temperature to 250 °C). The effective ("nominal") coating thickness was monitored by quartz microweights.

The emission properties of the samples were tested in an experimental apparatus assembled on the basis of a TCH-2 vacuum installation at a residual gas pressure of about 10^{-7} Pa. The device contained six identical sections and allowed parallel testing of the corresponding number of samples. Each of them was fixed on a separate object table equipped with a direct-glow heater, thanks to which the temperature of the sample could be adjusted in the range from the room temperature to 600 °C. The electric field was created in a planar gap of 0.6 mm wide between the sample and the end face of a cylindrical anode with a diameter of 6 mm.

After installing a batch of samples in the device and pre-pumping it, they were decontaminated by heating up to 150 °C. Further, the procedure of thermal field activation of the emission properties of coatings, developed earlier in the course of experiments with nanocarbon emitters, could be carried out [24]. For metal films, the parameters of the procedure were optimized by the selection method.

When measuring the emission characteristics, a slowly varying voltage was applied between the sample and the anode, up to a maximum value of 4.5 kV from a controlled high-voltage source. The time intervals of its rise and fall (linear in time) were 35 s, which corresponds to a frequency of 14 mHz. The voltage $U(t)$ and the emission current $I(t)$ were recorded by a digital oscilloscope and used to obtain the emission characteristics $I(U)$.

The samples of the coatings that passed the emission tests were studied using an atomic force microscope (AFM) of NanoDST Pacific Nanotechnology (USA) in so-called semi-contact (CloseContact) mode. This made it possible to determine the "true" topography of the surface with absolute values of the normal coordinate in the course of operational measurements under non-vacuum conditions, with minimal influence of the adsorbed layers of atmospheric gases and water on the measurement results. However, to remove an excessively dense layer of volatile substances, some samples were heated in air up to a temperature above 100 °C for 2 hours before performing AFM measurements. In addition to AFM, in some cases, a MIAIA3 Tescan scanning electron microscope (SEM) (Czech Republic) with the possibility of EMF analysis of the surface elemental composition was used.

The choice of the set of experimental methods used in the described primary experiments made it possible to conduct rapid testing of a large number of samples that differed in the material of metal coatings, their thickness, the parameters of the deposition processes and the type of substrate.

Experimental results

Emission properties of the samples and the possibility of their activation.

Experiments with the samples of metal coatings on silicon substrates confirmed the ability of some of these samples to emit electrons in an electric field with a macroscopic strength E (defined as the ratio of the applied voltage to the width of the field gap) of the order of units V/μm. The measured emission characteristics (Fig. 1) were usually exponential in the "straight" $I(U)$ coordinates and were well approximated by the linear dependence in the Fowler-Nordheim coordinates

$$\ln(I/U^2) = f(1/U),$$

This is considered to be a confirmation of the field (tunnel) nature of the emission mechanism.

As for the previously studied nanocarbon materials [24], the emissivity of metal films could be activated by applying the following thermal-field treatment procedure.

An electric field of low intensity (about 1 V/m) was applied to the sample, and the sample was heated at a rate of about 5 °C/min until an emission current of 100 nA appeared; or, in the absence of a field, until the temperature of 600 °C was reached (the point at which the thermal emission current appeared).

For many coatings, the auto-emission current appeared and began to increase over time

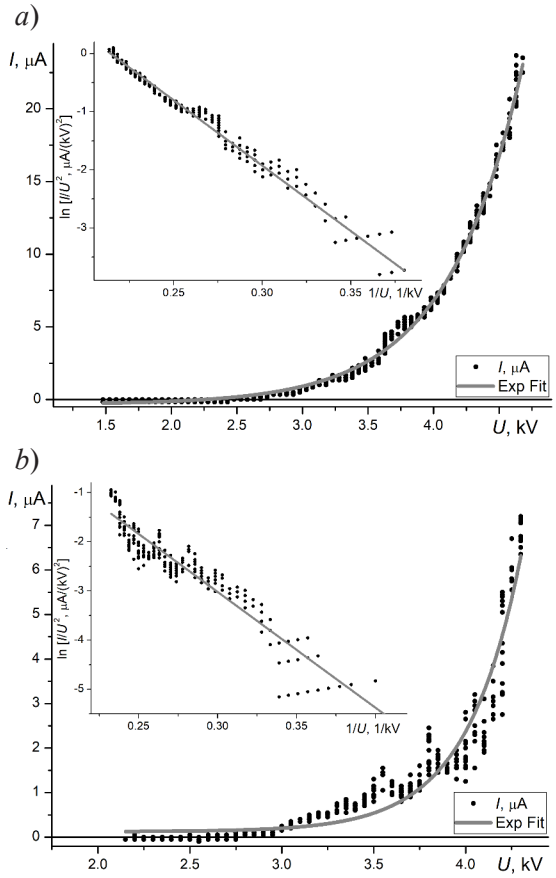

Fig.1. Emission characteristics of Mo (*a*) and Zr (*b*) film samples with an effective thickness of 6 nm. The insets show the same dependencies in Fowler – Nordheim coordinates

at a temperature of about 300 °C. After reaching the current value of 100 nA, the field strength was being gradually reduced, the current being kept at the specified value; at the same time the heating of the sample stopped, and, as the result, the sample slowly cooled to room temperature, while the value of the emission current at 100 nA level was still maintained (for this purpose, the voltage applied to the field gap was specially selected).

Due to the application of the described procedure to the samples with the best emission properties, the voltage level required to get the current of a given value was reduced several times. Attempts to simplify the procedure, for example, to activate the sample without applying an electric field, but only by temperature action, or to turn off the field during the cooling of the activated samples, were unsuccessful. Their result was invariably the loss of the emissivity of the studied structures.

The table summarizes the results of experiments on the influence of various parameters of thin metal films on their emissivity. The following sections of the article are devoted to a more complete description of them.

The emissivity of the samples (the best of the corresponding series) is characterized in the table by two values. One of them is the threshold value of the macroscopic field strength E_{th}, which was determined by the moment of the appearance of a current equal to about 100 nA. The other is the maximum value of the current $I_{\max}$, which could be taken from the sample area located opposite the anode (its diameter was 6 mm).

Comparison of the emission properties of thin films of different metals. To determine the effect of the coating material on emission, samples of films of five different metals were made: molybdenum, zirconium, nickel, tungsten and titanium, having the same nominal thickness d_{nom} (given in

Table

The main parameters of the studied films and their emission properties

Experiment No.	Material		Deposition rate, Å/s	E_{th}, V/μm	I_{max}, mkA
	Of the coating (d_{nom}, nm)	of the substrate			
1	Mo (6)	KDB 10	0.2	3.0	2.2
	Zr (6)		0.5	4.3	8.0
	Ni (6)		1.0	5.0	2.6
	W (6)		1.0	not determined	
	Ti (6)		0.2	no emission	
2	Mo (6)	Si + 200 nm of oxide	1.0	no emission	
	Mo (8)				
3	Mo (4)	KDB 10	0.2	4.8	0.05
	Mo (6)			3.0	2.20
	Mo (4)	KEF 7.5		4.0	0.15
	Mo (6)			6.4	0.03
4	Mo (2)	KDB 10	0.2	no emission	
	Mo (4)			not determined	
	Mo (6)			3.0	2.2
	Mo (8)		1.0	3.2	12
	Mo (10)			4.0	25
	Mo (20)			no emission	
5	Mo (6) № 1	KDB 10	0.13	3.2	4.16
	Mo (6) № 2		1.0	4.2	23.70
	Mo (6) № 3*			3.6	1.53

Designations: d_{nom} – nominal thickness of the metal film; KDB – boron-doped, hole-conducting silicon; KEF – phosphorus-doped silicon with electronic conductivity. Figures 7.5 or 10 mean the resistivity of the substrate, expressed in ohms per centimeter; E_{th} – the threshold electric field strength (determined by the moment of appearance of the current, equal to about 100 nA), I_{max} – the maximum emission current obtained.
Notes. The substrate temperature was 100 °C; the only exception was sample No. 3* in experiment 5, for which it was equal to 150°C.

the table in parentheses, in nm). A summary of the results of the comparison is also presented in the table.

The best emissivity was shown by the samples of molybdenum coatings (see Fig. 1,*a*). As a result, most of the experiments in this work were carried out with molybdenum films. Almost all the samples of Mo coatings with a nominal thickness in the range of 6 – 10 nm could emit electrons at a field strength of less than 10 V/μm. Figure 2,*a* shows a typical AFM image of a Mo coating with an effective thickness of 6 nm. From its appearance, it can be concluded that the coating is heterogeneous, while the average lateral size of the elevated areas ("islands") is close to 20 nm at their height of 1 – 2 nm. The density of the islands is about 500 μm^{-2}.

The zirconium films were characterized by similar surface topography. In a typical AFM image (Fig. 2,*b*), grains with an average transverse size of about 30 nm and a height of up to 2 nm are distinguishable; their distribution density is about 400 per μm^2. The emissivity of such films was noticeable even before the thermal field ac-

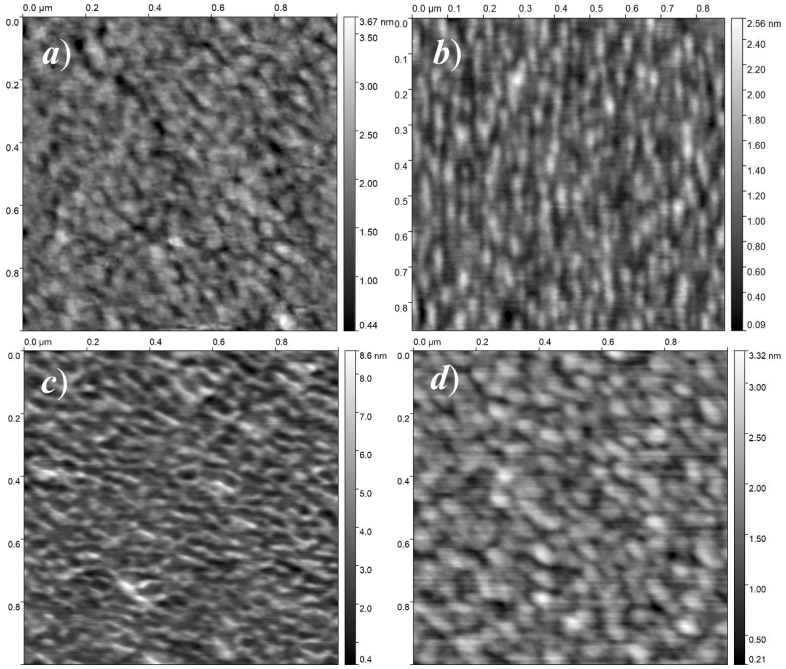

Fig. 2. AFM images of the surface of samples of metal coatings made of Mo (*a*), Zr (*b*), Ni (*c*), W (*d*) with an effective thickness of 6 nm

tivation procedure, and after the activation it was further improved (see Fig. 1,*b* and the table).

In terms of topography, the nickel film was markedly different from the metal films described above. The inhomogeneities present in the AFM images had a significantly larger vertical size and elongated shape. The length of the observed "elevations" for a typical case (see Fig. 2,*c*) reaches 60 – 100 nm at a height of up to 5 – 8 nm, and these elevations, as far as can be judged from the images, are assembled in a common network. Nickel films differed from those of molybdenum and zirconium in terms of their emission properties, and for the worse. After activation, they showed some emissivity, but the field emission current was extremely unstable. Upon reaching the value of 2 – 4 μA, the current irreversibly fell almost to zero; probably, a small number of emission centers on the surface were destroyed.

A typical AFM image of the surface of a tungsten film (Fig. 2,*d*) is similar in structure to images of molybdenum and zirconium. However, the topographical features here are somewhat larger: their transverse size is on average 80 nm, and their maximal height is about 3 nm. The emissivity of the tungsten films was worse than that of the metals considered earlier. When heated to 500 °C during the activation process, an emission current of 100 nA could be obtained at a voltage of 3.5 kV (at an emission gap of 0.6 mm). However, after cooling the sample, the threshold voltage values were above 4 kV, which made it technically impossible to register the emission dependences.

When analyzing the above experimental data, it should be taken into account that AFM images do not allow us to unambiguously determine whether the observed inhomogeneities of the topography are isolated islands of metal. The results of SEM-EMF mapping carried out for several samples indicate that metal coatings with a nominal thickness of 6 nm (or more) in the areas that were not damaged during the emission testing by the action of electric discharges (they were located outside the actively emitting areas), were solid. Consequently, in many cases, the obtained AFM images revealed only a local inhomogeneity of the film thickness, but not their separation into isolated islands, which could be expected due to the available data for carbon coatings with similar emission properties [17 – 19]. Nevertheless, the comparison of the emissivity of metal coat-

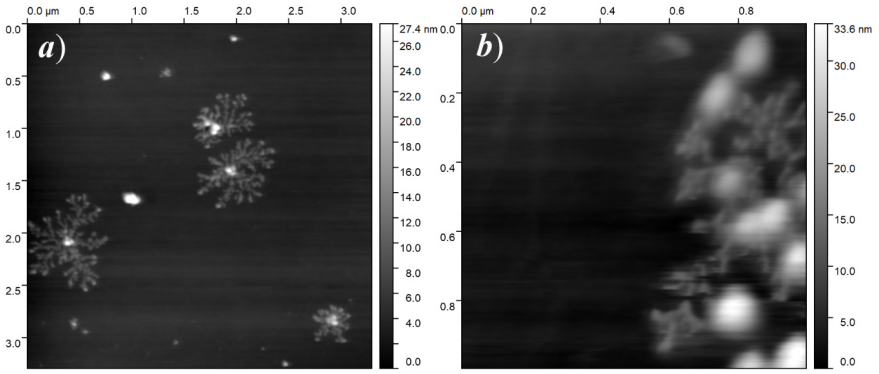

Fig. 3. AFM images of dendritic structures on the surfaces of two samples of coatings: Ti deposited on a Si plate without oxidation (*a*), and Mo deposited on a Si plate with a thick layer (about 200 nm) of oxide (*b*)

ings with the parameters of their AFM images revealed a significant correlation (confirmed by the results presented in the following sections): the best emissivity was possessed by the samples with the smallest scale of topographic surface heterogeneity.

The results of the experiment with titanium films deserve a separate discussion. They were distinguished by a complete lack of emissivity; the thermal field activation procedure also did not give the desired result. The image of the surface of one of the standard-made films of this metal is shown in Fig. 3,*a*. Here, the metal forms isolated islands of large size (in comparison with the grains of other coated films shown in Fig. 2), up to approximately 1 µm. The islands have a characteristic appearance of dendritic structures that "grow" from a central protrusion of considerable (tens of nanometers) height. There are no nanometer-sized islands here – this fact has been specially verified.

This morphology of the titanium film is unusual, since this metal is characterized in principle by high adhesion to silicon and its dioxide, which, in particular, allows the use of titanium layers as buffers when depositing films of other metals (see, for example, [25]). At the same time, it is known that the structure of titanium films significantly depends on the method and conditions of their applying [26]. The growth of dendrite-like ("fractal") clusters similar in shape and size to those found in our samples of titanium films (see Fig. 3), was observed and was theoretically described, for example, in [27]. To implement the mechanism of dendrite formation proposed there, it is required for the thin surface layer of the substrate to be non-conductive (usually the role of this layer is performed by the oxide), and for the deposited material to come in charged state. In this case, the field of accumulated surface charge prevents the deposition of new material in all areas, except for the vicinity of defects in the non-conducting layer, which defects allow the charge to "drain" into the volume of the substrate. This is just the place where the growth of the coating begins, spreading over the surface as a collection of dendritic structures that are electrically connected to the substrate through defects in the oxide layer.

For the conditions of applying titanium coating in this work, both criteria for the feasibility of the scenario described above could be met:

the natural oxide layer was preserved on the silicon substrates used;

when implementing the magnetron sputtering method, a significant part of the material comes to the substrate in the charged state [28].

The question of what particular features of the substrates, targets, or sputtering mode we used led to the formation of a titanium coating in the form of a set of dendrite-like islands requires further study. From the standpoint of the main goal of this study, the most important conclusion is that the titanium coating consisting of large dendrite clusters is not capable of low-threshold cold electron emission.

To test the assumption about the effect of the surface electric charging on the morphology

of the resulting films, a special experiment was performed (see experiment No. 2 in the table). The molybdenum films were deposited on silicon substrates with their own conductivity and on artificially oxidized surface. In the second case, the thickness of the oxide layer was 200 nm, which allowed us to expect an increase in the effects associated with surface charging, compared with the case of naturally oxidized substrates. Indeed, some areas of such coatings differed significantly in morphology from Mo films on silicon with a natural oxide layer (see Fig. 2,*a*) and were similar to Ti coatings (see Fig. 3,*a*): dendritic structures were formed on the surface, and they were "tied" to linear and point defects (see Fig. 3,*b*). Such samples showed no emissivity either before or during the thermal field activation procedure. In addition to the morphological features of the coatings, the absence of emission activity can also be attributed to the difficult transport of carriers to the emission centers through the thick oxide layer.

Dependence of the emission properties of coatings on the type of conductivity of the substrate

The nature of hot electron mechanism of emission suggests the possibility of a significant influence of the substrate properties on the emissivity. To assess experimentally the degree and nature of this effect, two molybdenum films with different values of effective thickness were grown on naturally oxidized substrates of *p*-type silicon of the KDB 10 brand and *n*-type silicon of the KEF 7.5 brand. Here Russian abbreviation KDB means boron-doped, hole-conducting silicon; KEF stands for "phosphorus-doped silicon with electronic conductivity"; figures mean the resistivity of the substrate, expressed in ohms per centimeter.

Summary data on the emissivity of such samples are given in the table (experiment No. 3). In general, we can note a slightly higher emissivity of films grown on substrates with hole conductivity. In addition, the samples of *n*-silicon substrates lost their emission properties after a short time (14 days) after the activation procedure. The best parameters were obtained from a sample of Mo-coating on a KDB 10 substrate, which had an effective layer thickness of 6 nm. It was characterized not only by a high emissivity, but also by the "correct" response to the thermal field activation procedure. Due to these properties, it is the substrates with hole conductivity that were used in most of the experiments in this work.

At the same time, the observed difference in the emissivity of the samples of different substrates could be determined not by the type of their conductivity itself, but by the morphology of the films created. AFM images of the surface of molybdenum coated samples with the same effective thickness of 6 nm on the substrates of different types are shown in Fig. 4. The differences in the topography of the films are quite noticeable: the coating grains on the *p*-Si substrate have smaller lateral dimensions (30 – 50 nm). The structure of the films having a surface with such

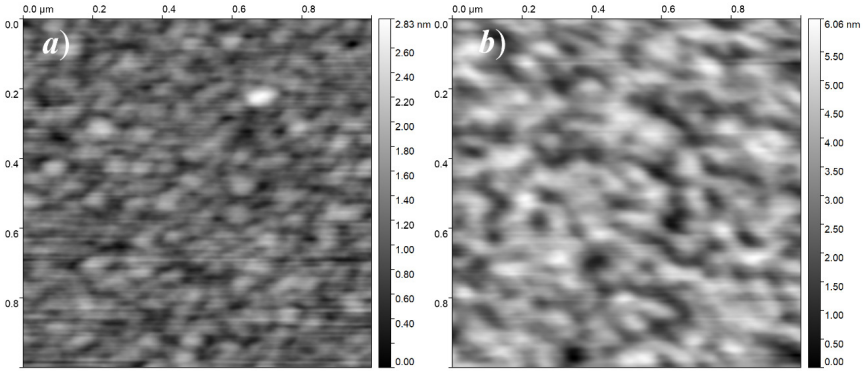

Fig. 4. AFM images of the surface of Mo films on KDB 10 (*a*) and KEF 7.5 (*b*) substrates. The effective thickness of the films is 6 nm

a topography was, in our conclusion, optimal in terms of their emissivity.

Dependence of the emission properties on the coating thickness

To clarify the relationship between the emission properties of coatings and their thickness, samples of molybdenum films with a nominal thickness of 2 to 20 nm were made on KDB 10 substrates. The summary of their best emission parameters is presented in the table (experiment No. 4).

For coatings with the thicknesses dnom of 2 and 4 nm, stable low-threshold emission could not be obtained. In contrast, coatings with nominal thickness of 6 nm showed low switching thresholds and stable emission current. However, the maximum values of the obtained current for them were small, and this may indicate a small number of activated emission centers. The 8 nm films were characterized by slightly higher threshold values of the electric field, but the maximum values of the I_{max} increased by more than 5 times, compared to the 6 nm films. Films with a nominal thickness of 10 nm had an even higher turning on threshold, but the maximum values of the obtained currents for them turned out to be the record for this type of structure studied by us. The sample with dnom = 20 nm had no emission properties at all; the procedure for its thermal field activation also did not bring the required results.

AFM images of the surface of Mo coatings of different thicknesses on substrates of the same type (KDB 10) are shown in Fig. 4,*a* and Fig. 5 (for the coating thickness of 6 nm). The pattern of regular changes in the surface topography of samples with an increase in the amount of deposited material is also illustrated by the graph in Fig. 6, which shows the dependence on the effective thickness of coatings for the "normalized roughness" of images calculated using the Gwyddion package.

In Fig. 5, *a*, which represents the coating of the smallest thickness (2 nm), only a few prominent features (grains) are found on the area of 1 μm^2 with a characteristic transverse size of up to 30 – 50 nm and the height of up to 1 – 2 nm. Approximately these are the dimensions of the islands, which, in accordance with the emission models used in the works [13 – 15, 20, 21], were associated with low-threshold field emission

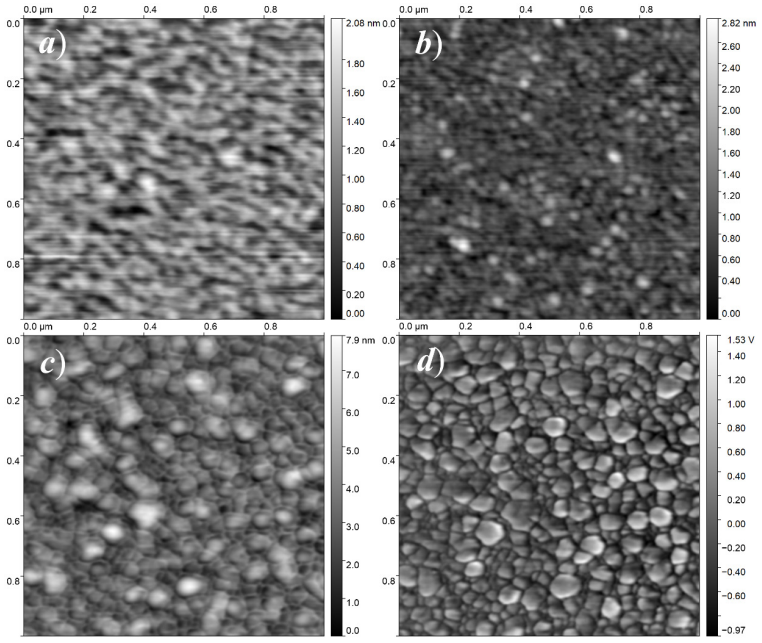

Fig. 5. AFM images of the surface topography of Mo films with different effective thicknesses, nm: 2 (*a*), 8 (*b*), 10 (*c*); *d* – "phase" image of the surface area (*c*). The films are grown on a KDB 10 substrate

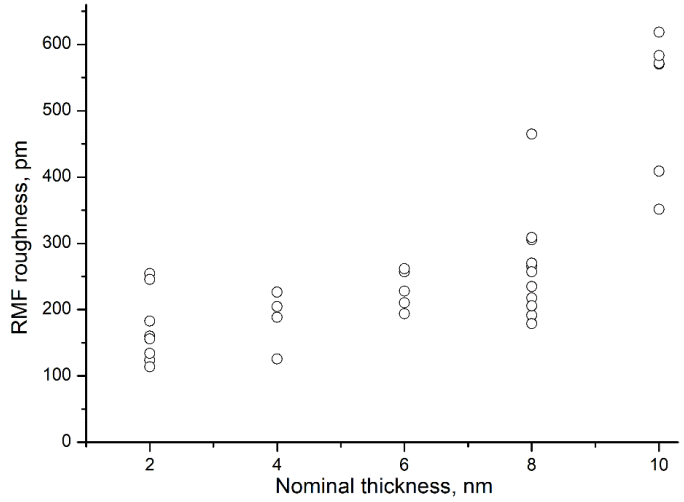

Fig. 6. Dependences of the root-mean-square parameter of the surface roughness of Mo films (according to AFM images) on the values of their effective thickness. Calculated using the Gwyddion package

centers. On the surfaces of d_{nom} = 6 nm and 8 nm (see Fig. 4,*a*, and 5,*b*, respectively) grains of the same size are present in much larger quantities, which may determine the high emissivity of such films. At the same time, AFM images of the 10 nm film (see the topography of the sample surface in Fig. 5,*c* and the corresponding "phase" distribution in Fig. 5,*d*) show a coating composed of contiguous domains of slightly larger transverse size and height. However, the grains of the size that we have defined as "optimal" are also present here. The smaller number of them can be responsible for the higher field emission threshold in such coatings, while the greater stability and endurance of the emission can be determined just by the presence of slightly larger islands. With further increase in the thickness of the Mo coating (sample 20 nm), the crystallites apparently formed a stable multilayer structure, and the film lost its emissivity.

Dependence of the emission properties on the parameters of the film deposition process

The experimental results described above indicate that the emission properties of coatings are related to their morphology. It is known that the morphology of coatings can change with varying conditions of their deposition. That is why in the course of this work, the coatings were compared, which differed only in the features of the technology of their growing. For comparison, Mo films with dnom = 6 nm grown on silicon substrates with hole conductivity were selected. The parameters of the manufacturing process of three such samples are given in the table (experiment No. 5). The topography of the surface of the obtained films is shown in the SEM images (Fig. 7).

On the surface of the sample No. 1 (see Fig. 7,*a*), formed at a temperature of 100 °C and the lowest growth rate (0.13 Å/s), grains with a typical transverse size of 20 nm were present. Their density can be estimated as approximately 500 μm^{-2}. In the image of sample No. 2 (Fig. 7,*b*), formed at the same temperature, but at a higher deposition rate, the grains have a larger average size: 30 – 40 nm; their number per unit area was approximately 300 μm^{-2}. Sample No. 3 (Fig. 7,*c*) was formed at an elevated substrate temperature (150 °C) and high film growth rate (1 Å/s). The average grain size here was the smallest one (about 15 – 20 nm) with a wide size distribution. The grain concentration was approximately 700 μm^{-2}.

Thus, it is obvious that there is a difference in the morphology of the coatings, and the grain variety, presumably associated with low-threshold emission centers, was present on the surface in all cases.

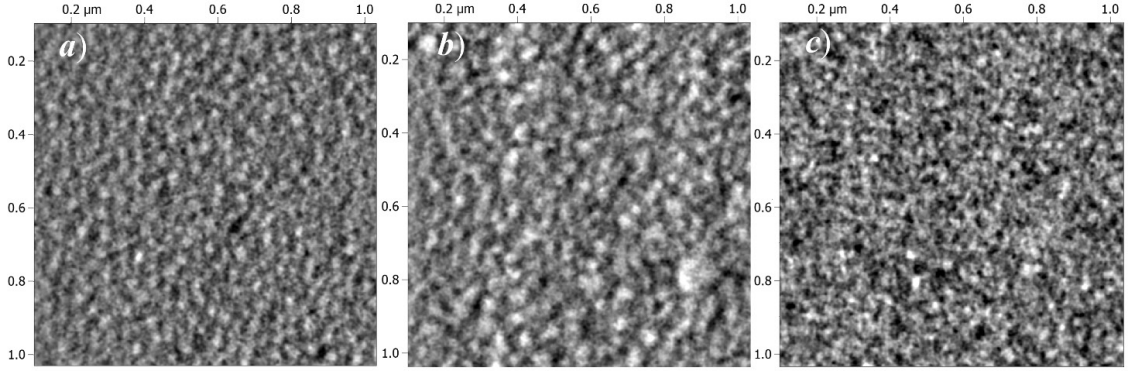

Fig. 7. SEM images (secondary electron detector) for samples No.1 (*a*), No.2 (*b*) and No.3 (*c*) made under different conditions (see experiment No. 5 in the table and description in the text)

In accordance with this, all three samples had the ability to emit electrons at low voltage with a noticeable quantitative difference in the emission parameters (see experiment No. 5 in the table). The correlation of the surface topography of the samples with their emissivity corresponded to the trends noted earlier.

The sample No. 1 with the smallest spatial scale of heterogeneity was characterized by the lowest emission threshold.

The threshold field for sample No. 2, with the largest grains, was the highest, but the maximum value of the sampled current I_{max} was also the highest (the current-voltage characteristic of the emission is shown in Fig. 1,*a*).

Sample No. 3 demonstrated the lowest value of the permissible emission current and intermediate values of the threshold field.

Discussion of the results and conclusions

The main result of the presented work can be considered as the fact of detection of low-voltage electron emission by thin metal films formed on oxidized silicon.

Then, the correlation of the film's emissivity with its morphology (as far as it can be estimated through AFM data) is established. At the same time, the influence of other factors, namely, the type of metal and the type of conductivity of the substrate, was weaker.

In the experiments carried out, the effectiveness of thermopole activation of auto-emissivity was confirmed for the case of metal coatings deposited on the semiconductor substrate. Just the same procedure was proposed earlier for carbon films [24]. This activation is largely analogous to the "electroforming" procedure required (according to the review [13] and the works mentioned there) to observe the emission of electrons from metal films when surface current flows through them. The physical content of this process is presumably metal atom migration, leading to the formation of isolated islands up to 100 nm in size, separated by gaps, on which, when a lateral potential difference appears, the electric field is concentrated. When electric current flows, the charge carriers cross the gaps between the islands by tunneling, which creates favorable conditions for the formation of population of hot electrons that can be emitted into vacuum. The effect is enhanced by the suppression of the electron-phonon interaction in nanoscale islands [13 – 15, 20, 21]. At the initial stages of the proposed thermal field activation procedure, the increased temperature accelerates the surface migration of atoms and promotes the formation of islands. It is known from the literature that thin solid metal films deposited on dielectric substrates at low temperature acquire an island structure as a result of heating to 300 – 600 °C [29]. In the presented experiments, to initiate the process of activating the emission properties of most coatings, they needed to be heated to a temperature from the same range. After the appearance of the emission current, the formation of the optimal coating structure can

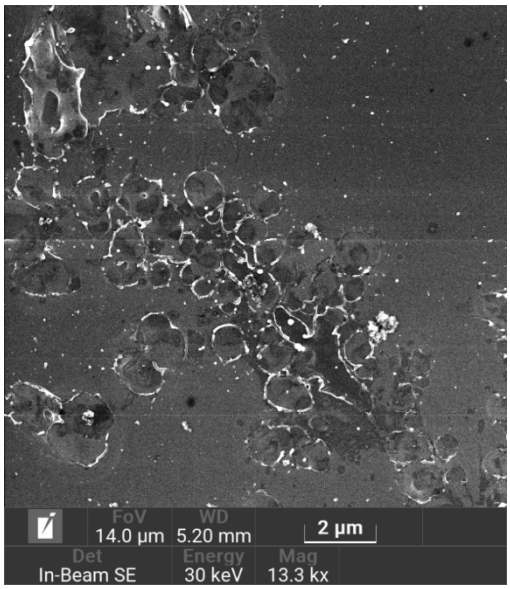

Fig. 8. SEM image of the surface of the Mo coating sample with the thickness of 10 nm after emission tests

be facilitated by additional factors caused by this current, namely, by local heating and ion bombardment of the surface; it was previously shown [30, 31] that irradiation with ion fluxes also contributes to the transformation of thin solid metal films into island films (dewetting). The possibility of forming coverage areas (emission centers) with a structure that is optimal in terms of the efficiency of heating the electronic subsystem of the islands and the emission of electrons into vacuum, should be determined, first of all, by the thickness of the metal film and its original morphology – the size and concentration of the crystallites already present in the composition. This is exactly what was observed in the experiments.

Among other things, the above hypothesis about the mechanism of activation of the emissivity of the studied coatings explains the small values of obtained emission currents, which did not exceed tens of microamperes when the current was collected from an area of about 0.3 cm^2. If the action of factors associated with the flow of the emission current causes an increase in the emission capacity of the local coating area, then a positive feedback between the emission current and the emission capacity is created, which should lead to the rapid destruction of most emission centers. (And indeed, the SEM images (Fig. 8) of the surface of the samples that had passed the emission tests often showed a large number of craters that can be identified with destroyed emission centers, even if no field gap breaks were recorded during testing.)

Due to the fact that the emerging emission centers are constantly activated until self-destruction, the lifetime of most of them is small. This limits the number of simultaneously functioning emission centers and the average value of the current density. Perhaps, the prospects for achieving high values of the average density of the emission current of cold film emitters should be associated with finding a way to control local emission currents – for example, with the introduction of microelectrode systems or resistive ballast layers.

REFERENCES

1. **Eletskii A.V.,** Carbon nanotube-based electron field emitters, Physics–Uspekhi. 53 (9) (2010) 863–892.

2. **Egorov N., Sheshin E.,** Field emission cathode-based devices and equipment. In: Field Emission Electronics. Springer Series in Advanced Microelectronics, Vol. 60. Springer, Cham, 2017.

3. **Egorov N.V., Sheshin E.P.,** On the current state of field-emission electronics, J. Surf. Invest.: X-ray, Synchrotron Neutron Tech. 11 (2) (2017) 285–294.

4. **Giubileo F., Di Bartolomeo A., Iemmo L., et al.,** Field emission from carbon nanostructures, Appl. Sci. 8 (4) (2018) 526.

5. **Fursey G.N.,** Field emission in vacuum microelectronics, Kluwer Academic–Plenum Publishers, New York, 2005.

6. **Fursey G.N., Polyakov M.A., Bagraev N.T., et al.,** Low-threshold field emission from carbon structures, J. Surf. Invest.: X-ray, Synchrotron Neutron Tech. 13 (5) (2019) 814–824.

7. **Kleshch V.I., Smolnikova E.A., Orekhov A.S.,**

et al., Nano-graphite cold cathodes for electric solar wind sail, Carbon. 81 (January) (2015) 132–136.

8. **Haque A., Narayan J.,** Electron field emission from Q-carbon, Diam. Relat. Mater. 86 (June) (2018) 71–78.

9. **Davidovich M.V., Yafarov R.K.,** Pulsed and static field emission VAC of carbon nanocluster structures: experiment and its interpretation, Tech. Phys. 64 (8) (2019) 1210–1220.

10. **Borzjak P.G., Sarbej O.G., Fedorowitsch R.D.,** Neue Erscheinungen in sehr dünnen Metallschichten, Phys. Status Solidi, B. 8 (1) (1965) 55–58.

11. **Nepijko S.A., Kutnyakhov D., Protsenko S.I., et al.,** Sensor and microelectronic elements based on nanoscale granular systems, J. Nanopart. Res. 13 (12) (2011) 6263–6281.

12. **Shen Z., Wang X., Wu S., Tian J.,** Numerical analysis of the surface-conduction electron-emitter with a new configuration, Mod. Phys. Lett. B. 30 (10) (2016) 1650137.

13. **Fedorovich R.D., Naumovets A.G., Tomchuk P.M.,** Electron and light emission from island metal films and generation of hot electrons in nanoparticles, Phys. Rep. 328 (2–3) (2000) 73–179.

14. **Bilotsky Y., Tomchuk P.M.,** Peculiarity of electron-phonon energy exchange in metal nanoparticles and thin films, Surf. Sci. 602 (1) (2008) 383–390.

15. **Tomchuk P., Bilotsky Y.,** New peculiarity in the temperature and size dependence of electron-lattice energy exchange in metal nanoparticles, Int. J. Mod. Phys. B. 28 (31) (2014) 1450220.

16. **Gloskovskii A., Valdaitsev D.A., Cinchetti M., et al.,** Electron emission from films of Ag and Au nanoparticles excited by a femtosecond pump-probe laser, Phys. Rev. B. 77 (19) (2008) 195427.

17. **Arkhipov A.V., Gabdullin P.G., Gordeev S.K., et al.,** Photostimulation of conductivity and electronic properties of field-emission nanocarbon coatings on silicon, Tech. Phys. 62 (1) (2017) 127–136.

18. **Andronov A., Budylina E., Shkitun P., et al.,** Characterization of thin carbon films capable of low-field electron emission, J. Vac. Sci. Technol. B. 36 (2) (2018) 02C108.

19. **Gabdullin P., Zhurkin A., Osipov V., et al.,** Thin carbon films: correlation between morphology and field-emission capability, Diam. Relat. Mater. 105 (May) (2020) 107805.

20. **Arkhipov A.V., Zhurkin A.M., Kvashenkina O.E., et al.,** Electron overheating during field emission from carbon island films due to phonon bottleneck effect, Nanosystems: Physics, Chemistry, Mathematics. 9 (1) (2018) 110–113.

21. **Arkhipov A.V., Eidelman E.D., Zhurkin A.M., et al.,** Low-field electron emission from carbon cluster films: combined thermoelectric/hot-electron model of the phenomenon, Fuller. Nanotub. Car. N. 28 (4) (2020) 286–294.

22. **Dubois S.M.-M., Zanolli Z., Declerck X., Charlier J.-C.,** Electronic properties and quantum transport in graphene-based nanostructures, Eur. Phys. J., B. 72 (1) (2009) 1–24.

23. **Varlamov A.A., Kavokin A.V., Luk'yanchuk I.A., Sharapov S.G.,** Anomalous thermoelectric and thermomagnetic properties of graphene, Physics–Uspekhi. 55 (11) (2012) 1146–1151.

24. **Bondarenko V.B., Gabdullin P.G., Gnuchev N.M., et al.,** Emissivity of powders prepared from nanoporous carbon, Tech. Phys. 49 (10) (2004) 1360–1363.

25. **Thomsen L.B., Nielsen G., Vendelbo S.B., et al.,** Electron emission from ultralarge area metal-oxide-semiconductor electron emitters, J. Vac. Sci. Technol. B. 27 (2) (2009) 562–567.

26. **Arshi N., Lu J., Lee C.G., et al.,** Thickness effect on properties of titanium film deposited by d.c. magnetron sputtering and electron beam evaporation techniques, Bull. Mater. Sci. 36 (5) (2013) 807–812.

27. **Mishin M.V., Zamotin K.Y., Protopopova V.S., Alexandrov S.E.,** Atmospheric pressure PECVD nanoparticles: Mechanism of nanoparticle self-organisation into micron sized fractal clusters on a solid surface, Phys. Chem. Chem. Phys. 17 (11) (2015) 7138–7148.

28. **Kashtanov P.V., Smirnov B.M., Hippler R.,** Magnetron plasma and nanotechnology, Physics–Uspekhi. 50 (5) (2007) 455–488.

29. **Niekiel F., Schweizer P., Kraschewski S.M., et al.,** The process of solid-state dewetting of Au thin films studied by in situ scanning transmission electron microscopy, Acta Mater. 90 (15 May) (2015) 118–132.

30. **Lo Savio R., Repetto L., Guida P., et al.,** Control of the micrometric scale morphology of silicon nanowires through ion irradiation-induced metal dewetting, Solid State Commun. 240 (Au-

gust) (2016) 41–45.

31. **Tuzhilkin M.S., Bespalova P.G., Mishin M.V., et al.,** Formation of Au nanoparticles and features of etching of a Si substrate under irradiation with atomic and molecular ions, Semiconductors. 54 (1) (2020) 137–143.

Received 14.10.2020, accepted 24.11.2020.

THE AUTHORS

BIZYAEV Ivan S.
Peter the Great St. Petersburg Polytechnic University
29 Politechnicheskaya St., St. Petersburg, 195251, Russian Federation
ivanbiziaev@yandex.com

GABDULLIN Pavel G.
Peter the Great St. Petersburg Polytechnic University
29 Politechnicheskaya St., St. Petersburg, 195251, Russian Federation
gabdullin_pg@spbstu.ru

GNUCHEV Nikolay M.
Peter the Great St. Petersburg Polytechnic University
29 Politechnicheskaya St., St. Petersburg, 195251, Russian Federation
nmg@rphf.spbstu.ru

ARKHIPOV Alexander V.
Peter the Great St. Petersburg Polytechnic University
29 Politechnicheskaya St., St. Petersburg, 195251, Russian Federation
arkhipov@rphf.spbstu.ru

СПИСОК ЛИТЕРАТУРЫ

1. **Елецкий А.В.** Холодные полевые эмиттеры на основе углеродных нанотрубок // УФН. 2010. Т. 180. № 9. С. 897–930.

2. **Егоров Н.В., Шешин Е.П.** Автоэлектронная эмиссия. Принципы и приборы. М.: Интеллект, 2011. 704 с.

3. **Егоров Н.В., Шешин Е.П.** Современное состояние автоэмиссионной электроники // Поверхность. Рентгеновские, синхротронные и нейтронные исследования. 2017. № 3. С. 5–15.

4. **Giubileo F., Di Bartolomeo A., Iemmo L., Luongo G., Urban F.** Field emission from carbon nanostructures // Applied Sciences. 2018. Vol. 8. No. 4. P. 526.

5. **Fursey G.N.** Field emission in vacuum microelectronics. New York: Kluwer Academic–Plenum Publishers, 2005, 205 p.

6. **Фурсей Г.Н., Поляков М.А., Баграев Н.Т., Закиров И.И., Нащекин А.В., Бочаров В.Н.** Низкопороговая полевая эмиссия из углеродных структур // Поверхность. Рентгеновские, синхротронные и нейтронные исследования. 2019. № 9. С. 28–39.

7. **Kleshch V.I., Smolnikova E.A., Orekhov A.S., Kalvas T., Tarvainen O., Kauppinen J., Nuottajarvi A., Koivisto H., Janhunen P., Obraztsov A.N.** Nano-graphite cold cathodes for electric solar wind sail // Carbon. 2015. Vol. 81. January. Pp. 132–136.

8. **Haque A., Narayan J.** Electron field emission from Q-carbon // Diamond and Related Materials. 2018. Vol. 86. June. Pp. 71–78.

9. **Давидович М.В., Яфаров Р.К.** Импульсные и статические автоэмиссионные ВАХ углеродных нанокластерных структур: эксперимент и

его интерпретация // Журнал технической физики. 2019. Т. 89. № 8. С. 1282–1293.

10. **Borzjak P.G., Sarbej O.G., Fedorowitsch R.D.** Neue Erscheinungen in sehr dünnen Metallschichten // Physica Status Solidi. B. 1965. Vol. 8. No. 1. Pp. 55–58.

11. **Nepijko S.A., Kutnyakhov D., Protsenko S.I., Odnodvorets L.V., Schönhense G.** Sensor and microelectronic elements based on nanoscale granular systems // Journal of Nanoparticle Research. 2011. Vol. 13. No. 12. Pp. 6263–6281.

12. **Shen Z., Wang X., Wu S., Tian J.** Numerical analysis of the surface-conduction electron-emitter with a new configuration // Modern Physics Letters. B. 2016. Vol. 30. No. 10. P. 1650137.

13. **Fedorovich R.D., Naumovets A.G., Tomchuk P.M.** Electron and light emission from island metal films and generation of hot electrons in nanoparticles // Physics Reports. 2000. Vol. 328. No. 2–3. Pp. 73–179.

14. **Bilotsky Y., Tomchuk P.M.** Peculiarity of electron-phonon energy exchange in metal nanoparticles and thin films // Surface Science. 2008. Vol. 602. No. 1. Pp. 383–390.

15. **Tomchuk P., Bilotsky Y.** New peculiarity in the temperature and size dependence of electron-lattice energy exchange in metal nanoparticles // International Journal of Modern Physics. B. 2014. Vol. 28. No. 31. P. 1450220.

16. **Gloskovskii A., Valdaitsev D.A., Cinchetti M., et al.** Electron emission from films of Ag and Au nanoparticles excited by a femtosecond pump-probe laser // Physical Review. B. 2008. Vol. 77. No. 19. P. 195427.

17. **Архипов А.В., Габдуллин П.Г., Гордеев С.К., Журкин А.М., Квашенкина О.Е.** Фотостимуляция проводимости и электронные свойства автоэмиссионных наноуглеродных покрытий на кремнии // Журнал технической физики. 2016. Т. 86. № 12. С. 135–144.

18. **Andronov A., Budylina E., Shkitun P., Gabdullin P., Gnuchev N., Kvashenkina O., Arkhipov A.** Characterization of thin carbon films capable of low-field electron emission // Journal of Vacuum Science and Technology. B. 2018. Vol. 36. No. 2. P. 02C108.

19. **Gabdullin P., Zhurkin A., Osipov V., Besedina N., Kvashenkina O., Arkhipov A.** Thin carbon films: correlation between morphology and field-emission capability // Diamond and Related Materials. 2020. Vol. 105. May. P. 107805.

20. **Arkhipov A.V., Zhurkin A.M., Kvashenkina O.E., Osipov V.S., Gabdullin P.G.** Electron overheating during field emission from carbon island films due to phonon bottleneck effect // Наносистемы: физика, химия, математика. 2018. Т. 9. № 1. С. 110–113.

21. **Arkhipov A.V., Eidelman E.D., Zhurkin A.M., Osipov V.S., Gabdullin P.G.** Low-field electron emission from carbon cluster films: combined thermoelectric/hot-electron model of the phenomenon // Fullerenes, Nanotubes and Carbon Nanostructures. 2020. Vol. 28. No. 4. Pp. 286–294.

22. **Dubois S.M.-M., Zanolli Z., Declerck X., Charlier J.-C.** Electronic properties and quantum transport in graphene-based nanostructures // The European Physical Journal. B. 2009. Vol. 72. No. 1. Pp. 1–24.

23. **Варламов А.А., Кавокин А.В., Лукьянчук И.А., Шарапов С.Г.** Аномальные термоэлектрические и термомагнитные свойства графена // Успехи физических наук. 2012. Т. 182. № 11. С. 1229–1234.

24. **Бондаренко В.Б., Габдуллин П.Г., Гнучев Н.М., Давыдов С.Н., Кораблёв В.В., Кравчик А.Е., Соколов В.В.** Эмиссионные характеристики порошков из нанопористого углерода // Журнал технической физики. 2004. Т. 74. № 10. С. 113–116.

25. **Thomsen L.B., Nielsen G., Vendelbo S.B., Johansson M., Hansen O., Chorkendorff I.** Electron emission from ultralarge area metal-oxide-semiconductor electron emitters // Journal of Vacuum Science & Technology. B. 2009. Vol. 27. No. 2. Pp. 562–567.

26. **Arshi N., Lu J., Lee C.G., Yoon J.H., Koo B.H., Ahmed F.** Thickness effect on properties of titanium film deposited by d.c. magnetron sputtering and electron beam evaporation techniques // Bulletin of Materials Science. 2013. Vol. 36. No. 5. Pp. 807–812.

27. **Mishin M.V., Zamotin K.Y., Protopopova V.S., Alexandrov S.E.** Atmospheric pressure PECVD nanoparticles: Mechanism of nanoparticle self-organisation into micron sized fractal clusters on a solid surface // Physical Chem-

istry, Chemical Physics. 2015. Vol. 17. No. 11. Pp. 7138–7148.

28. **Каштанов П.В., Смирнов Б.М., Хипплер Р.** Магнетронная плазма и нанотехнология // Успехи физических наук. 2007. Т. 177. № 5. С. 473–510.

29. **Niekiel F., Schweizer P., Kraschewski S.M., Butz B., Spiecker E.** The process of solid-state dewetting of Au thin films studied by in situ scanning transmission electron microscopy // Acta Materialia. 2015. Vol. 90. 15 May. Pp. 118–132.

30. **Lo Savio R., Repetto L., Guida P., Angeli E., Firpo G., Volpe A., Ierardi V., Valbusa U.** Control of the micrometric scale morphology of silicon nanowires through ion irradiation-induced metal dewetting // Solid State Communications. 2016. Vol. 240. August. Pp. 41–45.

31. **Тужилкин М.С., Беспалова П.Г., Мишин М.В., Колесников И.Е., Карабешкин К.В., Карасев П.А., Титов А.И.** Формирование наночастиц Au и особенности травления подложки Si после облучения атомарными и молекулярными ионами // Физика и техника полупроводников. 2020. Т. 54. № 1. С. 90–96.

Статья поступила в редакцию 14.10.2020, принята к публикации 24.11.2020.

СВЕДЕНИЯ ОБ АВТОРАХ

БИЗЯЕВ Иван Сергеевич – *аспирант, научный сотрудник лаборатории «Самоорганизующиеся высокотемпературные наноструктуры» Санкт-Петербургского политехнического университета Петра Великого, Санкт-Петербург, Российская Федерация.*

195251, Российская Федерация, г. Санкт-Петербург, Политехническая ул., 29

ivanbiziaev@yandex.com

ГАБДУЛЛИН Павел Гарифович – *кандидат физико-математических наук, доцент Высшей инженерно-физической школы Санкт-Петербургского политехнического университета Петра Великого, Санкт-Петербург, Российская Федерация.*

195251, Российская Федерация, г. Санкт-Петербург, Политехническая ул., 29

gabdullin_pg@spbstu.ru

ГНУЧЕВ Николай Михайлович – *доктор физико-математических наук, профессор Высшей инженерно-физической школы Санкт-Петербургского политехнического университета Петра Великого, Санкт-Петербург, Российская Федерация.*

195251, Российская Федерация, г. Санкт-Петербург, Политехническая ул., 29

nmg@rphf.spbstu.ru

АРХИПОВ Александр Викторович – *доктор физико-математических наук, доцент Высшей инженерно-физической школы Санкт-Петербургского политехнического университета Петра Великого, Санкт-Петербург, Российская Федерация.*

195251, Российская Федерация, г. Санкт-Петербург, Политехническая ул., 29

arkhipov@rphf.spbstu.ru